Kinetic Model for Short-Cycle Bulk Styrene Polymerization through Bifunctional Initiators

M. A. VILLALOBOS,* A. E. HAMIELEC, and P. E. WOOD

McMaster Institute for Polymer Production Technology, McMaster University, Hamilton, Ontario, Canada L8S 4L7

SYNOPSIS

A model describing the kinetics of bulk styrene polymerization through bifunctional initiators has been developed. The diffusion-controlled propagation and termination reactions at high monomer conversions are modeled with the free volume theory for polymer solutions. Three different commercially available bifunctional initiators were experimentally evaluated for a wide range of polymerization conditions to study the effect of the reaction rate on the molecular weight and molecular weight distribution. The model predictions for the same polymerization conditions show excellent agreement with the experimental data, for the whole range of conversions, for both reaction rate and molecular weight distribution development, under all the conditions tested. It is demonstrated throughout this study that high molecular weights, very high reaction rates, and narrow molecular weight distributions can be achieved simultaneously by using bifunctional initiators. A comparison between monofunctionally initiated systems with the bifunctionally initiated ones shows that short-cycle reactions with reductions in polymerization time of up to 75% may be achieved with the bifunctional initiators for a wider range of conditions without significantly affecting the molecular weight and molecular weight distribution of the final product.

INTRODUCTION

The nature of free radical polymerization is such that high polymerization rates and molecular weights can often not be obtained simultaneously. The chemical structure of the monomer determines the range of values for the propagation rate constant which causes difficulty in the control of the propagation reaction and, therefore, of the regularity of the polymer chains formed. Moreover, since the growing chains are free radicals, very high termination rates occur and this restricts the possibility of increasing the polymerization rate if, at the same time, it is necessary to maintain high molecular weights of the product.[1] The well-known polymerization mechanism involving monofunctional initiators[2,3] explains the limited possibility of increasing the polymerization rate by increasing the initiation rate and the need to optimize the initiator concentration in order to control the desired molecular weight distribution. The initiation rate is established by the initiator decomposition kinetics, which sets the temperature limits for its effective use, and this depends on the chemical structure of the initiator and its efficiency. This initiation efficiency, in turn, depends on the nature of both initiator and monomer. Due to these limitations, the possibilities of increasing the productivity of a monofunctionally initiated polymerization process are limited.

In the last decade a definitive breakthrough of the above concept, brought about by the commercial introduction of diperoxide compounds to be used as bifunctional initiators in free radical polymerization, has opened a new alternative to increase the productivity of some polymerization processes.

These initiators, with sequential decomposition kinetics,[4,5] modify completely the traditional polymerization mechanism, allowing higher reaction rates without sensibly lowering the molecular weights of the final product when most of the polymer chains are formed by bimolecular termination and transfer to small molecules is negligible.

An understanding of the reaction mechanism in-

* To whom correspondence should be addressed.

Journal of Applied Polymer Science, Vol. 42, 629–641 (1991)

 CCC 0021-8995/91/030629-13$04.00

volved in free radical polymerization through bifunctional initiators explains the feasibility of simultaneously obtaining high polymerization rates with high molecular weights.

In order to optimize new routes of polymer synthesis with bifunctional initiators it is necessary to develop a quantitative kinetic model capable of accurately predicting both the reaction rate and molecular weight averages development with conversion, for the whole range of conversions and under different operational conditions. However, the only model at present in the literature, shows serious limitations in its prediction of molecular weights and molecular weight distribution at high conversions.[6,7]

In this article, a reaction mechanism for styrene free radical bulk polymerization through bifunctional initiators is proposed and a step-by-step description of the kinetic model developed using this mechanism with the method of moments, is given. The modeling of the diffusion-controlled propagation and termination reactions at high monomer conversions, based on the free volume theory, is discussed. The model predictions of conversion vs. time and molecular weights vs. conversion are compared with experimental data. Results for bifunctionally initiated systems are compared with those monofunctionally initiated to clearly show the advantages of the use of bifunctional initiators.

REACTION MECHANISM

The chemical structure of symmetric bifunctional initiators is given by eq. (1). Here R_1 and R_2 represent different hydrocarbon ligands, and O—O peroxide groups.

$$R_1\text{—O—O—}R_2\text{—O—O—}R_1 \qquad (1)$$

The peroxide groups in a diperoxide molecule can undergo homolytic rupture of the O—O bonds by increasing the energy of the system, via temperature, radiation, or otherwise. Equation (2) shows the primary homolysis of a diperoxide molecule.

$$R_1\text{—O—O—}R_2\text{—O—O—}R_1 \xrightarrow{K_d} R_1\text{—O}\cdot + R_1\text{—O—O—}R_2\text{—O}\cdot \qquad (2)$$

When a diperoxide molecule is to be used as an initiator for free radical polymerization the following symbols may be used

$$I \xrightarrow{K_d} R_{in}^{\cdot} + \tilde{R}_{in}^{\cdot} \qquad (3)$$

The formation of diradical species, by either the simultaneous decomposition of the two peroxide groups in a diperoxide molecule or the decomposition of the peroxide group in the radical R_{in}, formed in eq. (3), in a polymerizing system during the life time of the radical before termination, is considered negligible. A probability calculation of its existence, based on decomposition rate constants of the bifunctional initiators employed in this study (measured at high and effective temperatures) shows that, on average, only one out of 5 million molecules is likely to form a diradical specie at any time during polymerization.

Accordingly, the proposed polymerization mechanism, considering the characteristics of styrene free radical polymerization, is shown below by eqs. (4)–(16).

Thermal initiation:

$$3M \xrightarrow{K_{Th}} 2R_1^{\cdot} \qquad (4)$$

Chemical initiation:

$$I \xrightarrow{2K_{d1}} R_{in}^{\cdot} + \tilde{R}_{in}^{\cdot} \qquad (5)$$

$$R_{in}^{\cdot} + M \xrightarrow{K_1} R_1^{\cdot} \qquad (6)$$

$$\tilde{R}_{in}^{\cdot} + M \xrightarrow{K_2} \tilde{R}_1^{\cdot} \qquad (7)$$

$$\tilde{P}_r \xrightarrow{K_{d2}} R_{in}^{\cdot} + R_r^{\cdot} \quad (r \geq 2) \qquad (8)$$

$$\tilde{\tilde{P}}_r \xrightarrow{2K_{d2}} R_{in}^{\cdot} + \tilde{R}_r^{\cdot} \quad (r \geq 2) \qquad (9)$$

Propagation:

$$R_r^{\cdot} + M \xrightarrow{K_p} R_{r+1}^{\cdot} \quad (r \geq 1) \qquad (10)$$

$$\tilde{R}_r^{\cdot} + M \xrightarrow{K_p} \tilde{R}_{r+1}^{\cdot} \quad (r \geq 1) \qquad (11)$$

Termination:

$$R_r^{\cdot} + R_s^{\cdot} \xrightarrow{K_{tc}} P_{r+s} \quad (r, s \geq 1) \qquad (12)$$

$$R_r^{\cdot} + \tilde{R}_s^{\cdot} \xrightarrow{K_{tc}} \tilde{P}_{r+s} \quad (r, s \geq 1) \qquad (13)$$

$$\tilde{R}_r^{\cdot} + \tilde{R}_s^{\cdot} \xrightarrow{K_{tc}} \tilde{\tilde{P}}_{r+s} \quad (r, s \geq 1) \qquad (14)$$

Transfer to monomer:

$$R_r^{\cdot} + M \xrightarrow{K_{Tfm}} P_r + R_1^{\cdot} \quad (r \geq 1) \qquad (15)$$

$$\tilde{R}_r^{\cdot} + M \xrightarrow{K_{Tfm}} \tilde{P}_r + R_1^{\cdot} \quad (r \geq 1) \qquad (16)$$

Hence, the following species will be present at any time during the reaction:

$R_{in}^{\cdot}$: initiator radical,

$\tilde{R}_{in}^{\cdot}$: in. radical with one undecomposed peroxide,

$R_r^{\bullet}$: ($r \geq 1$) macroradical,

$\tilde{R}_r^{\bullet}$: ($r \geq 1$) macroradical with one undecomposed peroxide,

P_r: (R—R) dead polymer molecule,

$\tilde{P}_r$: (R—$\tilde{R}$) dead polymer with one undecomposed peroxide,

$\tilde{\tilde{P}}_r$: ($\tilde{R}$—$\tilde{R}$) dead polymer with two undecomposed peroxides.

($\sim$ undecomposed peroxide groups, — polymer chain)

From the above set of polymeric species $\tilde{P}_r$ and $\tilde{\tilde{P}}_r$ represent polymer molecules "temporarily dead," for they may undergo further decomposition of the remaining terminal peroxide groups.

To establish the above reaction mechanism the following assumptions were made: (i) Different thermal stabilities for both peroxide groups in the same bifunctional initiator molecule; (ii) thermal stability of undecomposed peroxide groups in polymer molecules is independent of their chain length; (iii) termination occurs only by the combination mechanism; and (iv) transfer to monomer is likely to occur with the same rate for both macroradicals with and without undecomposed peroxides regardless of the chain length.

KINETIC MODELING

The ith moment for the concentration distributions of polymeric species (dead and temporarily dead), and radicals (live polymer) are defined as:

$$Q_i = \sum_{r=1}^{\infty} r^i [P_r] \Big\} \text{dead polymer}$$

$$\left.\begin{aligned} \tilde{Q}_i &= \sum_{r=1}^{\infty} r^i [\tilde{P}_r] \\ \tilde{\tilde{Q}}_i &= \sum_{r=1}^{\infty} r^i [\tilde{\tilde{P}}_r] \end{aligned}\right\} \text{temporarily dead polymer}$$

$$\left.\begin{aligned} Y_i &= \sum_{r=1}^{\infty} r^i [R_r] \\ \tilde{Y}_i &= \sum_{r=1}^{\infty} r^i [\tilde{R}_r] \end{aligned}\right\} \text{live polymer}$$

The total concentration of radical species with and without undecomposed peroxide groups is defined as

$$Y_{T0} = Y_0 + \tilde{Y}_0$$

The radical balances for a batch reactor are developed from the reaction mechanism and the ith moment definition

For primary radicals:

$R_{in}^{\bullet}$:

$$\frac{1}{V}\frac{d([R_{in}^{\bullet}]V)}{dt} = 2fK_{d1}[I] + fK_{d2}\tilde{Q}_0 + 2fk_{d2}\tilde{\tilde{Q}}_0 - K_1[M][R_{in}^{\bullet}] - K_{tc}Y_{T0}[R_{in}^{\bullet}] \quad (17)$$

$\tilde{R}_{in}$:

$$\frac{1}{V}\frac{d([\tilde{R}_{in}^{\bullet}]V)}{dt} = 2fK_{d1}[I] - K_2[M][\tilde{R}_{in}^{\bullet}] - K_{tc}Y_{T0}[\tilde{R}_{in}^{\bullet}] \quad (18)$$

Order of magnitude estimates show that the bimolecular termination terms in eqs. (17) and (18) are negligible. By applying the steady state hypothesis (SSH) for radical concentrations, the above equations can be expressed as

$$[R_{in}^{\bullet}] = \frac{f(2K_{d1}[I] + K_{d2}(\tilde{Q}_0 + 2\tilde{\tilde{Q}}_0))}{K_1[M]} \quad (19)$$

$$[\tilde{R}_{in}^{\bullet}] = \frac{2fK_{d1}[I]}{K_2[M]} \quad (20)$$

From eqs. (19) and (20), the initiation rates are obtained for initiation by radicals with and without peroxide groups. Note that the rate of thermal initiation in eq. (21) is added to the initiation rate of radicals without undecomposed peroxides.

$$R_{Th} = 2K_{Th}[M]^3 \quad (21)$$

$$R_I = K_1[M][R_{in}^{\bullet}] = f(2k_{d1}[I] + K_{d2}(\tilde{Q}_0 + 2\tilde{\tilde{Q}}_0)) + R_{Th} \quad (22)$$

$$\tilde{R}_I = K_2[M][\tilde{R}_{in}^{\bullet}] = 2fK_{d1}[I] \quad (23)$$

In the above equations it was assumed that the initiator efficiency (f) is the same for initiator (I) and for macroinitiator molecules ($\tilde{P}_r$ and $\tilde{\tilde{P}}_r$).

For growing radicals:

$R_1^{\bullet}$:

$$\frac{1}{V}\frac{d([R_1^{\bullet}]V)}{dt} = R_I + K_{Tfm}[M]Y_{T0} - K_P[M][R_1^{\bullet}] - K_{tc}Y_{T0}[R_1^{\bullet} - K_{Tfm}[M][R_1^{\bullet}] \quad (24)$$

$R_r^{\bullet}$ $(r \geq 2)$:

$$\frac{1}{V}\frac{d([R_r^{\bullet}]V)}{dt} = f K_{d2}[\tilde{P}_r] + K_P[M]([R_{r-1}^{\bullet}] - [R_r^{\bullet}]) - K_{tc}Y_{T0}[R_r^{\bullet}] - K_{Tfm}[M][R_r^{\bullet}] \quad (25)$$

$\tilde{R}_1^{\bullet}$:

$$\frac{1}{V}\frac{d([\tilde{R}_i^{\bullet}]V)}{dt} = \tilde{R}_I - K_P[M][\tilde{R}_1^{\bullet}] - K_{tc}Y_{T0}[\tilde{R}_1^{\bullet}] - K_{Tfm}[M][\tilde{R}_1^{\bullet}] \quad (26)$$

$\tilde{R}_r^{\bullet}$ $(r \geq 2)$:

$$\frac{1}{V}\frac{d([R_r^{\bullet}]V)}{dt} = 2fK_{d2}[\tilde{\tilde{P}}_r] + K_P[M]([\tilde{R}_{r-1}^{\bullet}] - [\tilde{R}_r^{\bullet}]) - K_{tc}Y_{T0}[\tilde{R}_r^{\bullet}] - K_{Tfm}[M][\tilde{R}_r^{\bullet}] \quad (27)$$

The polymer balances for a batch reactor may be expressed as

P_r:

$$\frac{1}{V}\frac{d([P_r]V)}{dt} = \frac{1}{2}K_{tc}\sum_{s=1}^{r-1}[R_s^{\bullet}][R_{r-s}^{\bullet}] + K_{Tfm}[M][R_r^{\bullet}] \quad (28)$$

$\tilde{P}_r$:

$$\frac{1}{V}\frac{d([\tilde{P}_r]V)}{dt} = K_{tc}\sum_{s=1}^{r-1}[R_s^{\bullet}][\tilde{R}_{r-s}^{\bullet}] + K_{Tfm}[M][\tilde{R}_r^{\bullet}] - K_{d2}[\tilde{P}_r] \quad (29)$$

$\tilde{\tilde{P}}_r$:

$$\frac{1}{V}\frac{d([\tilde{\tilde{P}}_r]V)}{dt} = \frac{1}{2}K_{tc}\sum_{s=1}^{r-1}[\tilde{R}_s^{\bullet}][\tilde{R}_{r-s}^{\bullet}] - 2K_{d2}[\tilde{\tilde{P}}_r] \quad (30)$$

The long chain approximation (LCA) is assumed to be valid for monomer consumption. This implies that the monomer is considered to be consumed only by propagation reactions. Monomer consumption through initiation, thermal and chemical, and transfer to monomer is neglected. Thus the following balance for monomer applies for a batch reactor

$$\frac{1dN_M}{Vdt} = -K_P[M]Y_{T0} \quad (31)$$

The bifunctional initiator is only consumed by its homolysis reaction in eq. (5), its balance for a batch reactor being

$$\frac{1dN_I}{Vdt} = -2K_{d1}[I] \quad (32)$$

The sums of eqs. (24) and (25), as well as (26) and (27) equal the total radical concentration variation with respect to time, for radical with and without peroxide groups, respectively.

The differential equations representing the variation with respect to time of the moments of the radical concentration distribution are calculated by using the definition of the ith moment to integrate these sums over the whole range of r $(r \geq 1)$. Although several different moments can be used to characterize a given distribution, the zeroeth, first, and second moment are commonly used since they allow the further calculation of M_n and M_w. Higher order moments may be calculated to establish higher order molecular weights.

Zeroeth moment:

$$\frac{d(Y_0V)}{Vdt} = R_I + f K_{d2}\tilde{Q}_0 + K_{Tfm}[M]\tilde{Y}_0 - K_{tc}Y_{T0}Y_0 \quad (33)$$

$$\frac{d(\tilde{Y}_0V)}{Vdt} = \tilde{R}_I + 2f K_{d2}\tilde{\tilde{Q}}_0 - K_{tc}Y_{T0}\tilde{Y}_0 - K_{Tfm}[M]\tilde{Y}_0 \quad (34)$$

First moment:

$$\frac{d(Y_1V)}{Vdt} = R_I + f K_{d2}\tilde{Q}_1 + K_p[M]Y_0 + K_{Tfm}[M](Y_{T0} - Y_1) - K_{tc}Y_{T0}Y_1 \quad (35)$$

$$\frac{d(\tilde{Y}_1V)}{Vdt} = \tilde{R}_I + 2f K_{d2}\tilde{\tilde{Q}}_1 + K_p[M]\tilde{Y}_0 - K_{tc}Y_{T0}\tilde{Y}_1 - K_{Tfm}[M]\tilde{Y}_1 \quad (36)$$

Second moment:

$$\frac{d(Y_2V)}{Vdt} = R_I + f K_{d2}\tilde{Q}_2 + K_p[M](2Y_1 + Y_0) + K_{Tfm}[M](Y_{T0} - Y_2) - K_{tc}Y_{T0}Y_2 \quad (37)$$

$$\frac{d(\tilde{Y}_2V)}{Vdt} = \tilde{R}_I + 2f K_{d2}\tilde{\tilde{Q}}_2 + K_p[M](2\tilde{Y}_1 + \tilde{Y}_0) - K_{tc}Y_{T0}\tilde{Y}_2 - K_{Tfm}[M]\tilde{Y}_2 \quad (38)$$

The above differential equations can be simplified to a set of algebraic equations by applying the steady state hypothesis for radical concentration. Note that a further simplification has been made since $Y_2 \gg Y_1 \gg Y_0$ for both types of radicals.

$$Y_0 = \frac{R_I + f K_{d2}\tilde{Q}_0 + K_{Tfm}[M]\tilde{Y}_0}{K_{tc}Y_{T0}} \quad (39)$$

$$\tilde{Y}_0 = \frac{\tilde{R}_I + 2f\kappa_{d2}\tilde{\tilde{Q}}_0}{K_{Tfm}[M] + K_{tc}Y_{T0}} \quad (40)$$

$$Y_1 = \frac{R_I + fK_{d2}\tilde{Q}_1 + K_p[M]Y_0}{K_{Tfm}[M] + K_{tc}Y_{T0}} \quad (41)$$

$$\tilde{Y}_1 = \frac{\tilde{R}_I + 2fK_{d2}\tilde{\tilde{Q}}_1 + K_p[M]\tilde{Y}_0}{K_{Tfm}[M] + K_{tc}Y_{T0}} \quad (42)$$

$$Y_2 = \frac{R_I + fK_{d2}\tilde{Q}_2 + 2K_p[M]Y_1}{K_{Tfm}[M] + K_{tc}Y_{T0}} \quad (43)$$

$$\tilde{Y}_2 = \frac{\tilde{R}_I + 2fK_{d2}\tilde{\tilde{Q}}_2 + 2K_p[M]\tilde{Y}_1}{K_{Tfm}[M] + K_{tc}Y_{T0}} \quad (44)$$

The differential equations describing the variation with respect to time of the moments of the polymer concentration distributions can be calculated by applying the ith moment definitions, on the polymer balances [eqs. (28)–(30)], to integrate over the whole range of chain lengths ($r \geq 1$).

Zeroeth moment:

$$\frac{d(Q_0V)}{Vdt} = \frac{1}{2}K_{tc}Y_0^2 + K_{Tfm}[M]Y_0 \quad (45)$$

$$\frac{d(\tilde{Q}_0V)}{Vdt} = K_{tc}Y_0\tilde{Y}_0 + K_{Tfm}[M]\tilde{Y}_0 - K_{d2}\tilde{Q}_0 \quad (46)$$

$$\frac{d(\tilde{\tilde{Q}}_0V)}{Vdt} = \frac{1}{2}K_{tc}\tilde{Y}_0^2 - 2K_{d2}\tilde{\tilde{Q}}_0 \quad (47)$$

First moment:

$$\frac{d(Q_1V)}{Vdt} = K_{tc}Y_1Y_0 + K_{Tfm}[M]Y_1 \quad (48)$$

$$\frac{d(\tilde{Q}_1V)}{Vdt} = K_{tc}(Y_0\tilde{Y}_1 + Y_1\tilde{Y}_0) + K_{Tfm}[M]\tilde{Y}_1 - K_{d2}\tilde{Q}_1 \quad (49)$$

$$\frac{d(\tilde{\tilde{Q}}_1V)}{Vdt} = K_{tc}\tilde{Y}_1\tilde{Y}_0 - 2K_{d2}\tilde{\tilde{Q}}_1 \quad (50)$$

Second moment:

$$\frac{d(Q_2V)}{Vdt} = K_{tc}(Y_1^2 + Y_0Y_2) + K_{Tfm}[M]Y_2 \quad (51)$$

$$\frac{d(\tilde{Q}_2V)}{Vdt} = K_{tc}(Y_0\tilde{Y}_2 + 2Y_1\tilde{Y}_1 + Y_2\tilde{Y}_0) + K_{Tfm}[M]\tilde{Y}_2 - K_{d2}\tilde{Q}_2 \quad (52)$$

$$\frac{d(\tilde{\tilde{Q}}_2V)}{Vdt} = K_{tc}(\tilde{Y}_1^2 + \tilde{Y}_0\tilde{Y}_2) - 2K_{d2}\tilde{\tilde{Q}}_2 \quad (53)$$

The simultaneous solution of the system of algebraic equations, (39)–(44), and differential equations, (31), (32), and (45)–(53), necessary to simulate the process is achieved by the application of a numerical method. A standard library subroutine named LSODE, which uses a fifth/sixth order Runge–Kutte algorithm for the step-wise simultaneous integration of the ODEs for finite increments in time, was applied to obtain the absolute values of the moments of radical and polymer concentration distributions along with the monomer and initiator concentrations for every time increment. From these values the conversion and molecular weight averages development with time are calculated as

$$X(t) = \frac{[M]_0 - [M](t)}{[M]_0} \quad (54)$$

$$M_n(t) = \frac{MW_M(Q_1(t) + \tilde{Q}_1(t) + \tilde{\tilde{Q}}_1(t) + Y_1(t) + \tilde{Y}_1(t))}{(Q_0(t) + \tilde{Q}_0(t) + \tilde{\tilde{Q}}_0(t) + Y_0(t) + \tilde{Y}_0(t))} \quad (55)$$

$$M_w(t) = \frac{MW_M(Q_2(t) + \tilde{Q}_2(t) + \tilde{\tilde{Q}}_2(t) + Y_2(t) + \tilde{Y}_2(t))}{(Q_1(t) + \tilde{Q}_1(t) + \tilde{\tilde{Q}}_1(t) + Y_1(t) + \tilde{Y}_1(t))} \quad (56)$$

In high-conversion free radical polymerization, the termination reactions become diffusion controlled and the termination rate decreases considerably with increase in monomer conversion, with the consequent increase in the polymerization rate. It is well known that the bimolecular termination is chain length dependent and that the number-average termination constant can be used to model polymerization rate and number-average molecular weight.[8] The number-average termination constant has been used in the present model. A semi-empirical method, based on the free volume theory,[3] was employed to model the diffusion-controlled termination reactions as follows: At the beginning of the polymerization ($X = 0$), the value of the termination rate constant is given by the Arrhenius type expression

$$K_{tc0} = A_t\exp(-E_t/RT) \quad (57)$$

Upon polymerization, the free volume of the reaction mix, dependent on the volumes of monomer and polymer, and the total volume, is calculated as

$$VF_p(X) = (0.025 + \alpha_p(T - T_{g_p})) \times (Vp(X)/Vt) \quad (58)$$

Table I Experimental Design

Initiator	Concentration (mol/L)	Temperature (°C)
Lucidol (BPO)	0.010	90
		105
		120
D-162	0.005	90
		105
	0.010	120
Lupersol-256	0.005	80
		90
	0.010	100
Lupersol-331	0.005	100
		115
	0.010	130

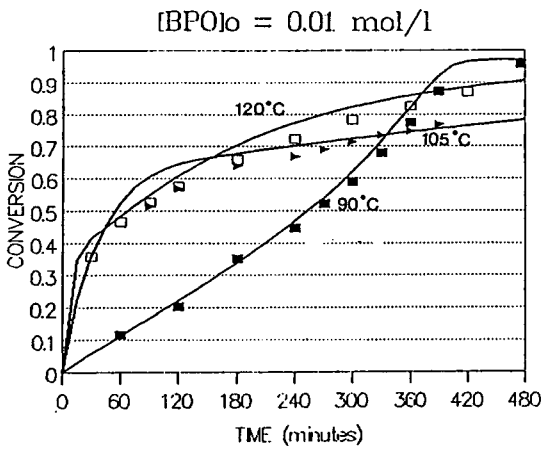

Figure 1 Effect of polymerization temperature on monomer conversion history with monofunctional initiator BPO 0.01 mol/L; (■, ▲, □) experimental data; (—) model prediction.

$$VF_m(X) = (0.025 + \alpha_m(T - T_{g_m})) \times (Vm(X)/Vt) \quad (59)$$

$$VF(X) = VF_p(X) + VF_m(X) \quad (60)$$

A critical value K_{cr} for the system is defined as a function of temperature. For every increment in conversion the parameter K is calculated as:

$$K(X) = M_w(X)^M \exp(A/VF(X)) \quad (61)$$

where M and A are adjustable parameters.

When $K \leq K_{cr}$ the termination rate constant is considered to increase linearly with conversion, due to increase in segmental diffusion rate of the polymer chains as the concentration of polymer in the system increases and the coil sizes decrease.

$$K_{tc}(X) = K_{tc0}(1 + \delta_T[P](X)) \quad (62)$$

At the conversion when K becomes greater than K_{cr}, VF, and M_w take their critical values and from then on K_{tc} is considered to decay exponentially as

Table II Model Values of the Kinetic Rate Constants

	$K_{Th} = 1.314 \times 10^7 \exp(-27440.5/RT)$	(l/min)
	$K_P = 6.128 \times 10^8 \exp(-7067.8/RT)$	(L/mol-min)
	$K_{tc} = 1.00 \times 10^{11} \exp(-1677.03/RT)$	(L/mol-min)
	$K_{Tfm} = 3.148 \times 10^{22} \exp(-37563.9/RT)$	(L/mol-min)
Initiator D-162:		
	$K_{d1} = 2.117 \times 10^{14} \exp(-28063.85/RT)$	(l/min)
	$K_{d2} = 3.850 \times 10^{20} \exp(-40{,}022.15/RT)$	(l/min)
Lupersol-256		
	$K_{d1} = 5.895 \times 10^{17} \exp(-32613.06/RT)$	(l/min)
	$K_{d2} = 1.246 \times 10^{31} \exp(-55868.48/RT)$	(l/min)
Lupersol-331-80B:		
	$K_{d1} = 1.269 \times 10^{18} \exp(-35662.08/RT)$	(l/min)
	$K_{d2} = 1.090 \times 10^{21} \exp(-42445.26/RT)$	(l/min)
	$f = 0.7$	
Gel-effect parameters:		
	$K_{cr} = 9.44 \exp(3833/RT)$	
	$\delta_T = 0.00$	
	M = 0.50	
	A = 0.25	
	N = 1.75	
	B = 1.00	

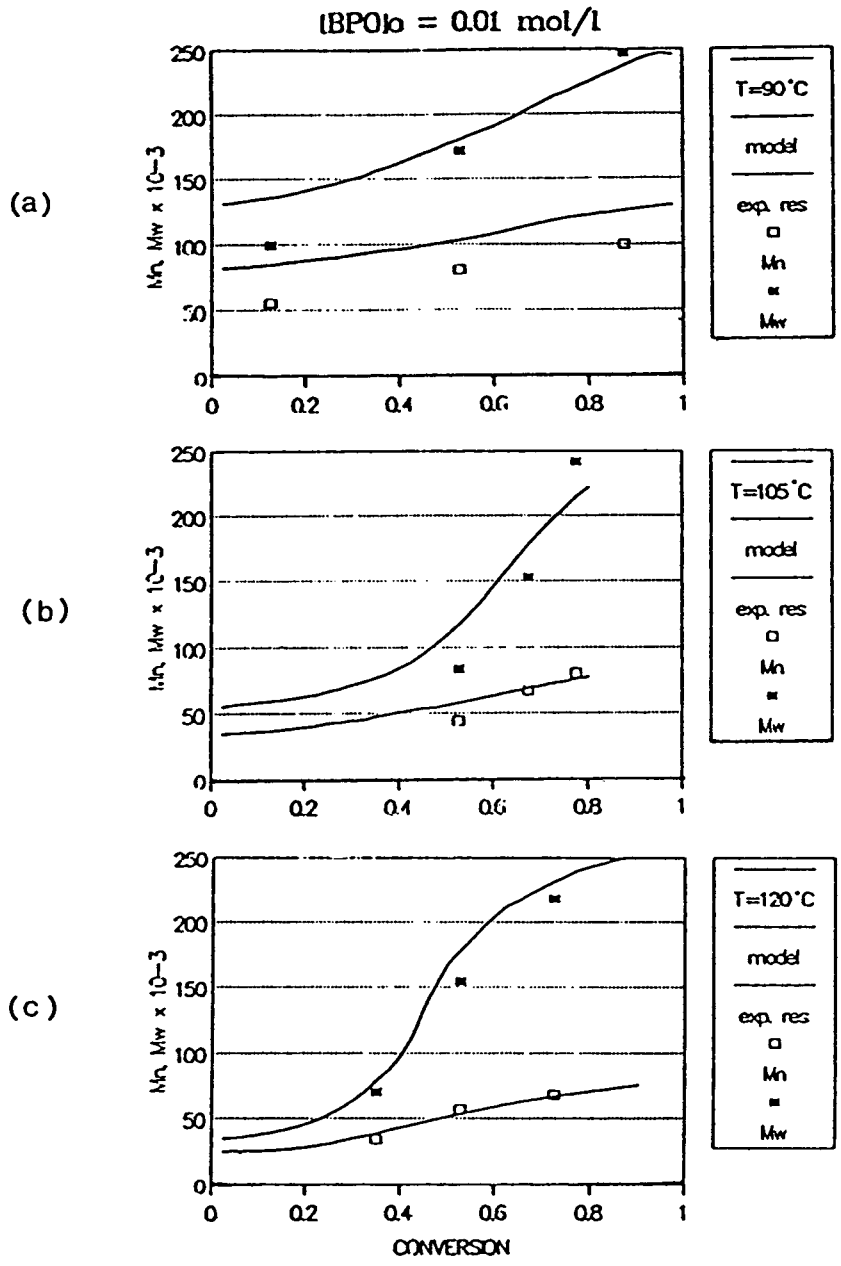

Figure 2 Effect of polymerization temperature on molecular weights and molecular weight distribution development with monofunctional initiator BPO 0.01 mol/L (■, □) experimental data; (—) model prediction.

$$K_{tc}(X) = K_{tc}(M_{w_{cr}}/M_w(X)^N \exp(-A(1/VF(X) - 1/VF_{cr}) \quad (63)$$

where N is an adjustable parameter.

Also, when a free radical polymerization is carried out at temperatures below the glass transition temperature (T_g) of the polymer being formed, the T_g of the reaction mixture ($T_{g_{mix}}$), which depends on conversion and molecular weight, equals the polymerization temperature (T_p) at a critical conversion X_{cr} and the polymerization rate falls to essentially zero ($K_p \approx 0$). For conversions higher than X_{cr}, therefore, the propagation reaction becomes diffusion controlled. This phenomenon is modeled by decreasing the propagation rate, for $X > X_{cr}$, as

$$K_p(X) = K_p \exp(-B(1/VF(X) - 1/VFp_{cr})) \quad (64)$$

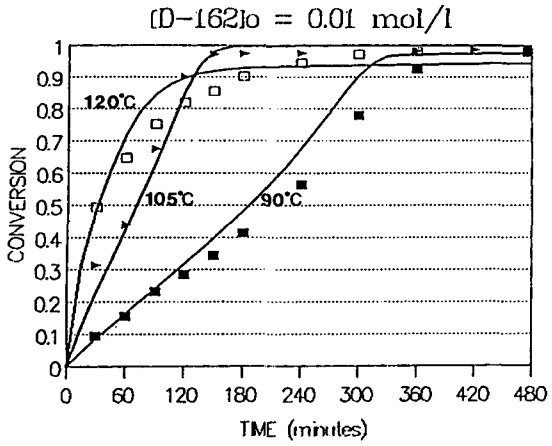

Figure 3 Effect of polymerization temperature on monomer conversion history with bifunctional initiator D-162 0.01 mol/L; (■, ▲, □) experimental data; (—) model prediction.

where B is an adjustable parameter. The adjustable parameters K_{cr}, M, A, N, and B may be established by any suitable optimized fit method against experimental data. The initiator efficiency also decays along with the propagation rate constant at these high conversions. Equation (64), in fact, correlates $Kp(f^i)$ vs. VF to account for this phenomenon.

EXPERIMENTAL

Styrene (Aldrich Chemical) was washed three times with double-fold excess of sodium hydroxide solution (5%), rinsed three times with deionized water, dried with calcium chloride, distilled under vacuum from cuprous chloride at 30–35°C, and stored at −5°C until used. The monofunctional initiator benzoyl peroxide (Lucidol-BPO) and bifunctional initiators 2,5-dimethyl-2,5-bis(2-ethylhexanoyl peroxy)-hexane (Lupersol-256) and 1,1-di(*t*-butyl peroxy)-cyclohexane (Lupersol-331-80B), were supplied by the Pennwalt–Lucidol Co. The bifunctional initiator 1,4-bis(*t*-butyl peroxycarbo)cyclohexane (initiator D-162), was supplied by Akzo Chemie. 1,4-Dioxane and methanol, both reactive grade, were used as solvent and nonsolvent for polystyrene, respectively, without any further purification. Isothermal bulk polymerizations of styrene were carried out in 5 mm (OD) glass ampoules. The ampoules were filled with the desired mixtures styrene/initiator (see Table I), and degassed on a vacuum system by four successive freeze–thaw cycles using liquid nitrogen and a maximum pressure of 10^{-4} Torr. The ampoules were sealed off from the vacuum system and immersed in a constant temperature oil bath, then quickly removed, at the previously selected sampling times, and quenched immediately in liquid nitrogen to completely stop polymerization.

Conversion of the ampoule contents were determined gravimetrically by dissolving the samples in 1,4 dioxane and precipitating the polymer with a 10-fold excess of methanol. The slurry was vacuum filtered and washed thoroughly with methanol. The polymer was recovered and dried under vacuum at 50°C for 24 h. The molecular weight distribution was determined by gel permeation chromatography using tetrahydrofuran as carrier solvent in a Waters Scientific Model-150C GPC/ALC, on samples having conversions closest to 0, 50, and 100%. Model predictions for the same experimental conditions contained in Table I were performed using the kinetic rate constants values given in Table II.

DISCUSSION OF RESULTS

The effect of polymerization temperature on polymerization rate and molecular weight distribution development, for monofunctionally initiated styrene bulk polymerizations, was studied first. Figure 1 shows the limited range of polymerization temperatures in which BPO is effective. For polymerization at 90°C this initiator has its most effective decomposition rate and a conversion of 96% was reached after 8 h. As can be seen in Figure 2(a), under these conditions, M_n = 100,000 and M_w = 247,000 were experimentally obtained with a polydispersity index (PD = M_w/M_n) of 2.47. Higher polymerization temperatures caused the system to run out of initiator, after a very high initial polymerization rate, and lower terminal conversions were reached (Fig. 1). For these inefficient polymerizations, higher molecular weights were obtained at terminal conversion, along with broad molecular weight distributions, PD > 3 [Figs. 2(b) and 2(c)]. The predictions performed with the model for bifunctionally initiated systems, assuming a very high value for K_{d2} to simulate monofunctional initiation, show excellent agreement with the experimental results for conversion vs. time and good agreement (maximum deviations, 10%) for molecular weight distribution development with conversion. From these results it may be clearly seen that for monofunctionally initiated free radical polymerizations, shorter polymerization cycles cannot be achieved by increasing the polymerization temperature without affecting the molecular weight distribution of the product, due to the narrow range of applicability of these initia-

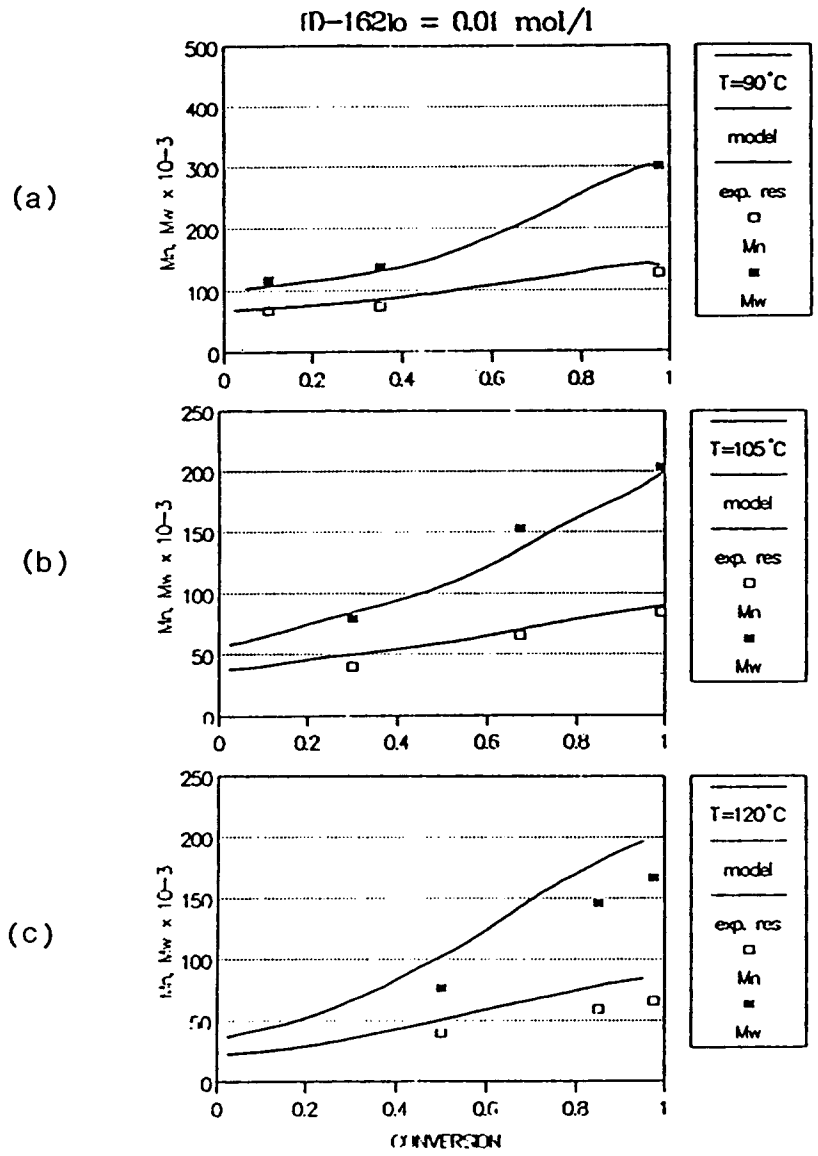

Figure 4 Effect of polymerization temperature on molecular weights and molecular weight distribution development with bifunctional initiator D-162 0.01 mol/L; (■, □) experimental data; (—) model prediction.

tors. As it is well known higher polymerization rates may be achieved by increasing the initiator concentration but lower molecular weights are also obtained.

The effect of temperature on monomer conversion and molecular weight development with conversion, for bulk styrene polymerization with bifunctional initiators, showed that initiator D-162 was the one that had most advantages as a substitute for BPO. While this initiator is effective for a wide range of moderate polymerization temperatures (90–105°C), bifunctional initiator Lupersol-256 has a narrower range of applicability around 90°C, and Lupersol-331-80B is effective for higher polymerization temperatures (100–130°C). Polymerization cycles ranging from 2 to 5 h were achieved with bifunctional initiator D-162, with the product having conversion levels greater than 97% (Fig. 3).

The weight average molecular weights reached with bifunctional initiator D-162 for the polymerization cycles of 2 and 5 h were 203,000 and 301,000, with polydispersity indices of 2.36 and 2.42, respectively [Fig. 4(a) and (b)]. These results demonstrate that the molecular weight distribution in free radical polymerization through bifunctional initiators is controlled by the polymerization rate. The

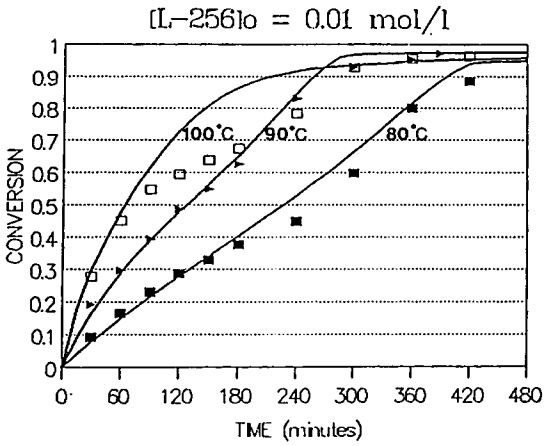

Figure 5 Effect of polymerization temperature on monomer conversion history with bifunctional initiator Lupersol-256 0.01 mol/L; (■, ▲, □) experimental data; (—) model prediction.

higher the polymerization rate the narrower is the molecular weight distribution obtained.

Bifunctional initiator Lupersol-256 gave its best performance at 90°C where a polymerization cycle of 5 h was achieved (Fig. 5). The conversion vs. time curve for this initiator at the lowest temperature tested (80°C) showed two different slopes at low and intermediate conversions due to the different decomposition characteristics of the two peroxide groups. At higher polymerization temperatures higher initial reaction rates were achieved and this effect was screened by the change in slope due to the auto-acceleration caused by the gel effect. As it can be seen in Figures 3 and 5, the effect of temperature on the terminal conversions reached at the end of the polymerizations carried out at temperatures below the T_g of polystyrene (below 100°C), the glassy effect limited the conversions to levels below 99%, while for those polymerizations carried out at T_p above 100°C the terminal conversions reached were close to 100%, provided the initiators were effective at those temperatures. The conversion curve with bifunctional initiator Lupersol-256 at 100°C (see Fig. 5), showed a drastic change in slope at high conversions. This result suggests that the reaction is first carried out at low conversions by the decomposition of the first peroxide in the molecule, which eventually runs out, and by the decomposition of the second peroxide during the last stages of the reaction.

The effect of temperature on molecular weights and molecular weight distribution development for bulk styrene polymerization with bifunctional initiator Lupersol-256, showed drastic increases for M_n and M_w that are caused by the successive termination and reinitiation reactions at lower polymerization rates. For polymerization with this initiator at 80°C a reaction cycle of 8 h was necessary to reach conversions above 90%, with the final product having M_w = 383,000 and PD = 2.87, while for the most efficient reaction with this initiator at 90°C, a total cycle of 6 h was achieved with the product having M_w = 338,000 and PD = 2.70 [see Figs. 5 and 6(a) and (b)]. Higher polymerization rates may be reached with this initiator at 90°C by increasing the initiator concentration to achieve shorter cycles with lower molecular weights and narrower molecular weight distributions.

Bifunctional initiator Lupersol-331-80B, although very effective in promoting higher reaction rates (polymerization cycles with this initiator ranged from 1.5 to 6 h as can be seen in Fig. 7), with high molecular weights for the product, under the whole range of temperatures tested (see Table I), requires higher polymerization temperature to be effective. This fact makes it more attractive for use

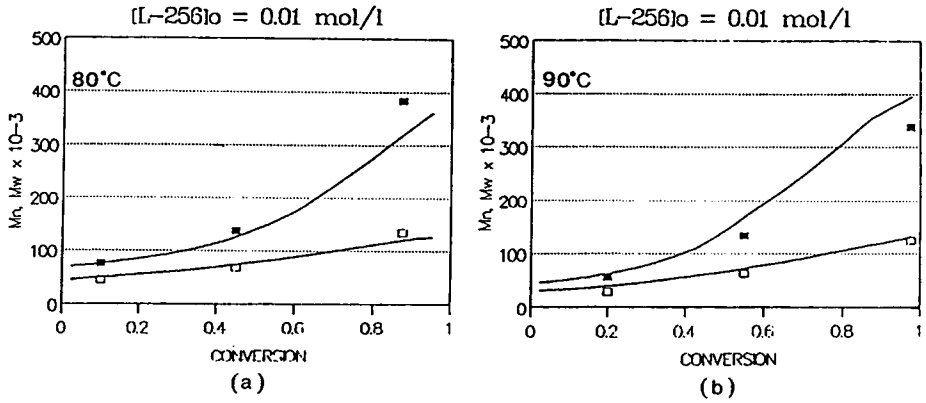

Figure 6 Effect of polymerization temperature on molecular weights and molecular weight distribution development with bifunctional initiator Lupersol-256 0.01 mol/l; (■, □) experimental data; (—) model prediction.

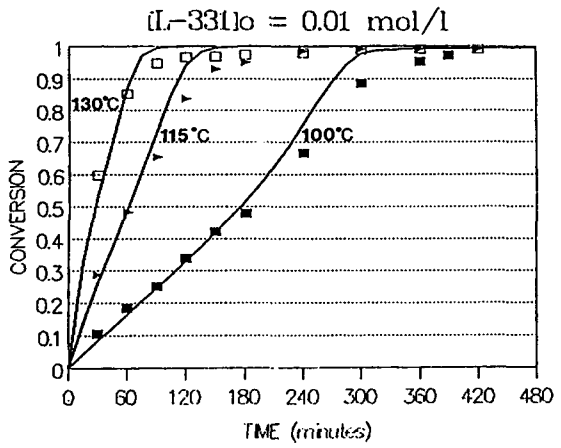

Figure 7 Effect of polymerization temperature on monomer conversion history with bifunctional initiator Lupersol-331-80B 0.01 mol/L; (■, ▲, □) experimental data; (—) model prediction.

as a finishing initiator than for carrying out reactions to high conversion levels. However, it may be used as principal initiator for PS synthesis with great advantages over the monofunctionally initiated system, if polymerization temperatures from 100 to 130°C are attempted. Since all the polymerizations with this bifunctional initiator were carried out at temperatures above the T_g of polystyrene no glassy effect was present at high monomer conversions, and terminal conversions close to 100% were achieved. The shortest polymerization cycle, 1.5 h, was obtained with this initiator at 130°C, with the final product having M_w = 179,000 with PD = 2.44 [Fig. 8(b)]. The narrowest molecular weight distribution (even narrower than those obtained with the monofunctionally initiated systems), was also achieved with this initiator at 100°C, M_w = 360,000 with PD = 2.21 [Fig. 8(a)]. These results show once more that very narrow molecular weight distributions may be achieved with bifunctional initiators when the polymerization conditions are properly selected to reach high initiator decomposition rates and therefore high polymerization rates.

The model predictions for the effect of temperature on conversion vs. time and molecular weight distribution development with conversion show excellent agreement for all three bifunctional initiators, in the whole range of conversions, under all the conditions tested.

The effect of initiator concentration on polymerization rate and molecular weight distribution was studied by decreasing the bifunctional initiator concentration to 0.005 mol/L. The expected behavior for the polymerization rate was observed for all three bifunctional initiators under all the temperatures tested (Figs. 9, 10, and 11). Lower initiator concentrations caused lower polymerization rates, longer polymerization cycles, lower terminal conversions, and higher molecular weights.

Bifunctional initiators D-162 and Lupersol-331-80B, were still effective for PS synthesis at this concentration, at 105 and 130°C, respectively, achieving shorter polymerization cycles, ranging from 3.5 to 6 h, in comparison to the 8 h with the monofunctional system. The same levels of molecular weights (M_w 250,000 to 300,000) and similar or even narrower molecular weight distributions (PD 2.38 to 2.65) were achieved under these conditions, as can be seen in Figure 12(a) and (b). Bifunctional initiator Lupersol-256 was not effective for PS synthesis at this low concentration. Lower terminal conversions and very high molecular weights were

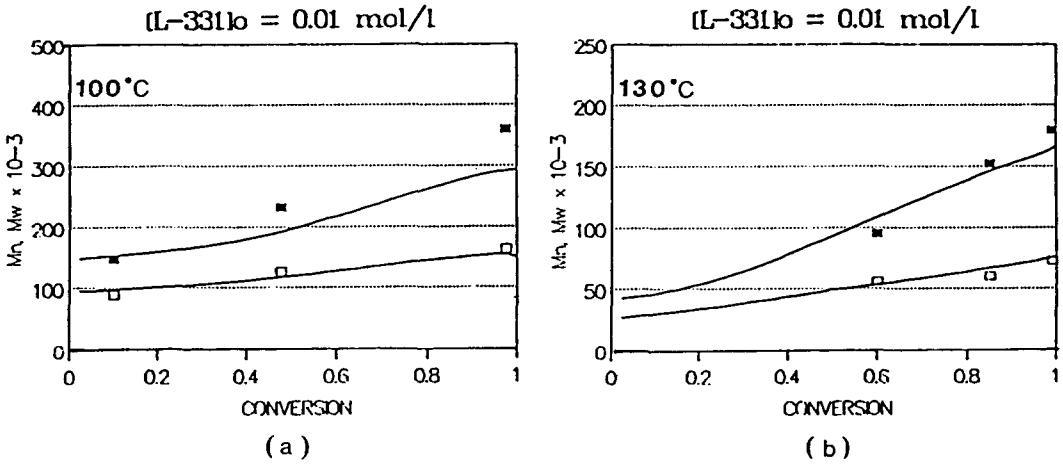

Figure 8 Effect of polymerization temperature on molecular weights and molecular weight distribution development with bifunctional initiator Lupersol-331-80B 0.01 mol/L; (■, □) experimental data; (—) model prediction.

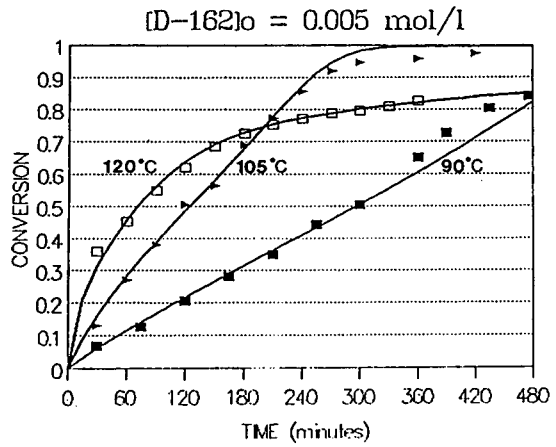

Figure 9 Effect of polymerization temperature on monomer conversion history with bifunctional initiator D-162 0.005 mol/L; (■, ▲, □) experimental data; (—) model prediction.

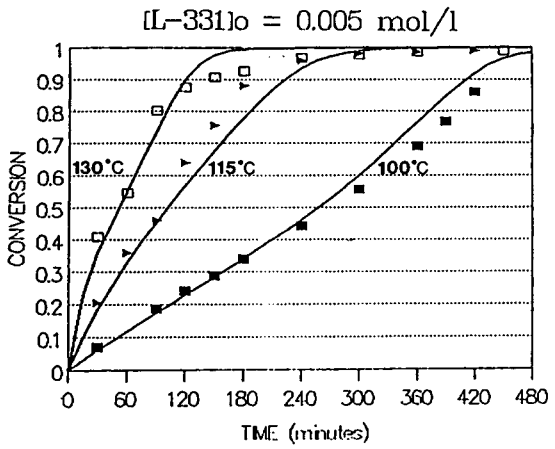

Figure 11 Effect of polymerization temperature on monomer conversion history with bifunctional initiator Lupersol-331-80B 0.005 mol/L; (■, ▲, □) experimental data; (—) model prediction.

obtained along with broader molecular weight distributions [Figs. 10 and 12(c) and (d)].

The model predictions for all of these experimental conditions also showed excellent agreement with the experimental data, in the whole range of conversions, for the three different temperatures, and bifunctional initiators tested. With this model, even the drastic increase in molecular weights caused by free radical polymerization with bifunctional initiators at low reaction rates was accurately predicted [Figure 12(d)].

CONCLUDING REMARKS

Herein is reported a reaction mechanism for free radical polymerization through bifunctional initiators along with a detailed description of the simulation model developed using this mechanism. The model developed for polystyrene takes into account thermal initiation and transfer to monomer reactions and uses the free volume theory to model the diffusion controlled propagation and bimolecular termination reactions at high monomer conversions. Extensive experimental data of conversion vs. time and molecular weight distribution development was presented for three different commercially available bifunctional initiators under a wide range of polymerization temperatures and initiator concentrations.

Taking as a reference polystyrene synthesis with the monofunctional initiator benzoyl peroxide at [I] = 0.01 mol/L and 90°C, it was demonstrated that reductions in polymerization cycle time by 20 to 75% may be achieved by using bifunctional initiators at the same or lower concentrations and at an adequate polymerization temperature. Under these conditions higher polymerization rates, high molecular weights, and narrow molecular weight distributions can be achieved simultaneously, to obtain final products with the same molecular weights and even narrower molecular weight distribution than with their monofunctionally initiated counterparts.

The reaction mechanism proposed explains how the molecular weight distribution for bifunctionally initiated systems depends on the relative concentration of growing free radical species with and without undecomposed terminal peroxide groups, which in turn depends on the polymerization rate. Therefore, molecular weight distributions may be tailored by selecting an adequate reaction rate with these bifunctionally initiated systems.

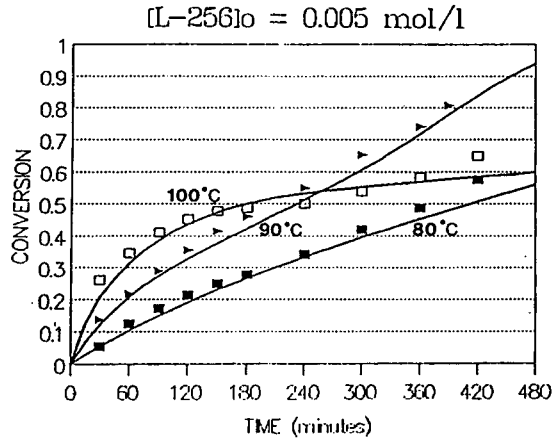

Figure 10 Effect of polymerization temperature on monomer conversion history with bifunctional initiator Lupersol-256 0.005 mol/L; (■, ▲, □) experimental data; (—) model prediction.

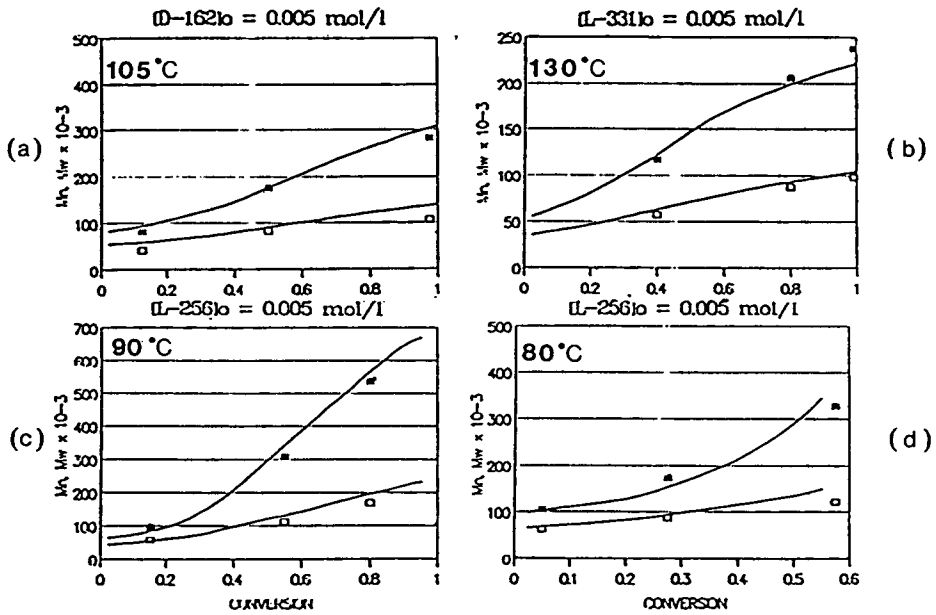

Figure 12 Effect of type of bifunctional initiator at low initiator concentration (0.005 mol/L) on molecular weights and molecular weight distribution development with: (a) Initiator D-162; (b) Lupersol-331-80B; (c) and (d) Lupersol-256; (■, □) experimental data; (—) model prediction.

The different decomposition kinetics of the two peroxide groups in a symmetrical bifunctional initiator is demonstrated by the two different slopes observed in conversion curves, at low polymerization rates. The model developed takes into account this change in the activation energy for the homolysis of the second peroxide group, that occurs only after the first peroxide has undergone homolysis. The change in reactivity between the two peroxide groups can also be explained in terms of different efficiencies for initiator and macroinitiator molecules, however, this model considers only the change in activation energy.

The simulation program BIFUN created from the model developed in this study predicts quite accurately both the reaction rate and molecular weight distribution development, in the whole range of conversions, under all the different conditions tested.

NOMENCLATURE

A	Frequency factor in Arrhenius equations
E	Activation energy
I	Initiator
M	Monomer
MW_M	Molecular weight of monomer
M_n	Number average molecular weight
M_w	Weight average molecular weight
P	Polymer
T_g	Glass transition temperature
VF	Free volume
X	Conversion
[ ]	Concentration
α_m	Thermal expansion coefficient for monomer
α_p	Thermal expansion coefficient for polymer
δ_T	Rate of increase in segmental diffusion

Subscripts:

m	Monomer
p	Polymer
t	Total
cr	Critical

REFERENCES

1. S. S. Ivanechev, *Polym. Sci. USSR*, **20**, 2157 (1979).
2. N. Friis and A. E. Hamielec, *J. Appl. Polym. Sci.*, **19**, 97 (1975).
3. F. L. Marten and A. E. Hamielec, *J. Appl. Polym. Sci.*, **27**, 489 (1982).
4. A. I. Prisyazhnyuk and S. S. Ivanechev, *Polym. Sci. USSR*, **12**, 514 (1970).
5. V. R. Kamath, Technical Data Report to Pennwalt–Lucidol Co. (1980).
6. K. Y. Choi and G. D. Lei, *AIChE J.*, **33**, 2067 (1987).
7. K. Y. Choi, W. R. Liang, and G. D. Lei, *J. Appl. Polym. Sci.*, **35**, 1547 (1988).
8. S. Zhu and A. E. Hamielec, *Macromolecules*, **22**, 3093 (1989).

Received March 7, 1990
Accepted April 17, 1990